Iterative Detection and ICI Cancellation for MISO-mode DVB-T2 System with Dual Carrier Frequency Offsets

Eun-Sung Jeon[1], Jeong-Wook Seo[2], Jang-Hoon Yang[3], Jong-Ho Paik[4] and Dong-Ku Kim[1]
[1] Department of Electrical and Electronic Engineering, Yonsei University
134 Sichon-dong, Seodaemun-gu, Seoul 120-749, Korea
[e-mail: youngmil2@yonsei.ac.kr, dkkim@yonsei.ac.kr]
[2] Advanced Mobile Technology Research Center, Korea Electronic Technology Institute
1599 Sangam-dong, Mapo-gu, Seoul 121-835, Korea
[e-mail: jwseo@keti.re.kr]
[3] Department of Newmedia, Korea German Institute of Technology
661 Deungchon-dong, Kangseo-gu, Seoul 157-030, Korea
[e-mail: jhyang@kgit.ac.kr]
[4] Multimedia Department, Seoul Women's University,
621 Hwarang-ro, Nowon-gu, Seoul 139-774, Korea
[e-mail: paikjh@swu.ac.kr]
*Corresponding author: Dong-Ku Kim

Received October 11, 2011; revised December 27, 2011; accepted January 27, 2012; published February 28, 2012

Abstract

In the DVB-T2 system with a multiple-input single-output (MISO) transmission mode, Alamouti coded orthogonal frequency division multiplexing (OFDM) signals are transmitted simultaneously from two spatially separated transmitters in a single frequency network (SFN). In such systems, each transmit-receive link may have a distinct carrier frequency offset (CFO) due to the Doppler shift and/or frequency mismatch between the local oscillators. Thus, the received signal experiences dual CFOs. This not only causes dual phase errors in desired data but also introduces inter-carrier interference (ICI), which cannot be removed completely by simply performing a CFO compensation. To overcome this problem, this paper proposes an iterative detection with dual phase errors compensation technique. In addition, we propose a successive-iterative ICI cancellation technique. This technique *successively* eliminates ICI in the initial iteration by exploiting pre-detected data pairs. Then, in subsequent iterations, it performs a fine interference cancellation using *a priori* information, *iteratively* fed back from the channel decoder. In contrast to previous works, the proposed techniques do not require estimates of dual CFOs. Their performances are evaluated via a full DVB-T2 simulator. Simulation results show that the DVB-T2 receiver equipped with the proposed dual phase errors compensation and the successive-iterative ICI cancellation techniques achieves almost the same performance as ideal dual CFOs-free systems, even for large dual CFOs.

Keywords: DVB-T2, MISO, OFDM, carrier frequency offset.

DOI: 10.3837/tiis.2012.02.015

1. Introduction

Digital video broadcasting–second generation terrestrial (DVB-T2) was published by the European Telecommunication Standard Institute (ETSI) in 2008 as the next generation broadcasting standard [1]. It is an extension of the television standard DVB-T and was developed for use in post-analog switch-off (ASO). As with DVB-T, DVB-T2 transmits signals using orthogonal frequency division multiplex (OFDM) modulation with concatenated channel coding and interleaving. It adopts the latest modulation and coding techniques to increase the transmission capacity. For error correction coding, DVB-T2 uses low-density parity-check (LDPC) coding combined with Bose–Chaudhuri–Hocquengham (BCH) coding. This offers powerful error correction capabilities, making it possible to use high-order modulation such as 256-quadrature amplitude modulation (QAM). To provide service-specific robustness, the concept of physical layer pipes (PLPs) is introduced. This enables different types of data to be transported independently, each with its own physical parameters (e.g., modulation, code rate, and interleaving depth). A new technique of constellation rotation and Q-delay provides significant robustness in difficult channels such as deep fading and impulsive noise channels. To reduce the overhead, several options are available in the fast Fourier transform (FFT) size, guard interval, and pilot patterns [2].

To improve coverage in a single frequency network (SFN), DVB-T2 can incorporate the option of multiple-input single-output (MISO)-mode using the Alamouti technique [3] in which the second remote transmitter transmits a slightly modified version of each pair of data subcarriers in the reverse order, as shown in **Fig. 1**. Because DVB-T2 is based on OFDM modulation, its performance is very sensitive to carrier frequency offset (CFO). CFO results in inter-carrier interference (ICI) by breaking the orthogonality between subcarriers. CFO occurs due to the Doppler shift and/or frequency mismatch between oscillators in the transmitter and the receiver. In DVB-T2, a special preamble called the P1 symbol is inserted at the beginning of every T2-frame in order to estimate the CFO. As shown in **Fig. 2**, the P1 symbol has a frequency-shifted guard interval at both ends to increase the correlation between the main part of the P1 symbol and the two intervals. The CFO estimation is carried out by correlating the received P1 symbol and by taking the argument of the correlator output' peak [2]. If DVB-T2 uses the MISO-mode in which signals are transmitted simultaneously from two spatially separated transmitters with their own oscillators, two distinct CFOs, i.e., dual CFOs, may exist in the received signal, one for each transmitter.

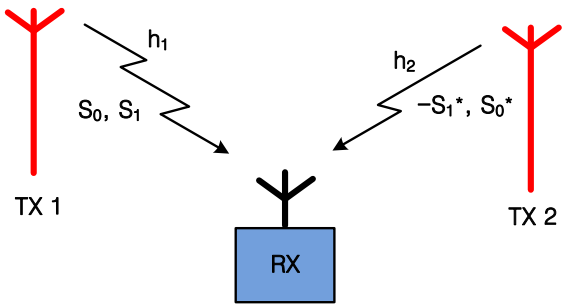

Fig. 1. MISO transmission mode [1]

The dual CFOs cannot be compensated completely by merely adjusting the compensation frequency at the receiver. Therefore, ICI always remains and thus, ICI mitigation methods are always required. Recently, various techniques have been proposed to mitigate the ICI occurring due to dual CFOs [4][5][6][7][8][9][10][11][12]13]. In [4], a frequency domain equalizer was proposed where the off-diagonal elements of the frequency domain channel matrix corresponding to the ICI are eliminated; this is similar to ICI cancellation for a single-input single-output (SISO) OFDM system. However, this approach suffers from performance loss in the high SNR region. In order to remove the error floor, an iterative decoding technique was proposed in [5], where the ICI terms in the channel matrix are gradually eliminated by iterations at the cost of increased complexity. To accomplish the trade-off between complexity and performance, a low complexity minimum mean-square error (MMSE)-based frequency domain equalization employing the ordered successive interference cancellation scheme is proposed in [6]. On the other hand, a time domain equalization using the Viterbi algorithm is proposed in [7]. A special two branches receiver architecture is proposed in [8], where the received signal is separately synchronized and decoded for each CFO. Then, out of two sets of decoded signals, more reliable signal is decided based on the minimum Euclidean distance decision criterion. In [9], the two branches receiver architecture is modified to combine the two separately synchronized signals, which leads to the increase of resulting signal to interference-plus-noise ratio (SINR) similarly to the maximum ratio combining (MRC) technique. In the area of asynchronous cooperative systems, a new space-time coding scheme is proposed in [10], where an OFDM symbol is modulated onto a group of subcarriers with proper weighting coefficient so that the ICI within the same group can be self-cancelled. Other researches on space-time encoded transmission schemes robust to dual CFOs are presented in [11][12][13]. Such previous works have assumed that perfectly estimated dual CFOs are given to the receiver.

Another problem occurring due to dual CFOs is that two distinct phase errors are introduced in the desired data, which results in subcarrier phase rotation. Unfortunately, these dual phase errors cannot be estimated by using conventional pilot-aided phase error estimation schemes such as those in [14][[15][16], because the components of two distinct phase errors are coupled with channel frequency responses. To our best knowledge, there is no literature dealing with the dual phase errors estimation scheme. In [17], an optimal dual CFOs compensation frequency is proposed which minimized the power of ICI. We noticed that when the compensation frequency is set to the optimized value, the components of the dual phase errors become a complex conjugate pair and can be separated from the channel frequency response. Based on this observation, we first propose the dual phase errors estimation scheme that exploits the binary phase-shift keying (BPSK)-modulated L1-pre data, and then compensates for the dual phase errors in conjunction with iterative data detection. We also propose a successive-iterative ICI cancellation technique that *successively* eliminates the ICI by using the pre-detected data pair in the initial iteration and from the second iteration, *a priori* information *iteratively* fed back from the LDPC decoder is used to accurately eliminate the ICI.

Contrary to previous works [4][5][6][7][8][9][10][11][12][13], our work *do not* assume that estimates of dual CFOs are given to the receive since estimating the dual CFOs can be an impossible task for DVB-T2. This is because the P1 correlator provides a *single* CFO estimate by processing the sum of two concurrently received P1 symbols, which is neither of the dual CFOs. To obtain the estimates of dual CFOs, two transmitters should send P1 symbols alternately during two time slots. In other words, one transmitter sends a P1 symbol and estimates its own CFO during the P1 symbol decoding process, while the other is set to zero,

i.e., a null P1 symbol. However, this decreases the data rate and is also practically impossible for application to current systems. This motivates us to explore new approaches to combat dual CFOs for DVB-T2 application.

This paper is organized as follows: Section 2 describes the model of DVB-T2 transmit and received signals. Section 3 first analyzes the effect of dual CFOs on the desired data and then presents iterative data detection with the proposed dual phase errors compensation technique. Section 4 proposes the successive-iterative ICI cancellation technique. Numerical results are presented in Section 5, and finally, the conclusions are given in Section 6.

2. System Model

2.1 Transmit Signal Model

The DVB-T2 signal consists of super frames that are divided into T2-frames, as shown in **Fig. 2**. Each T2-frame is composed of OFDM symbols, including P2 symbols and data symbols. The P2 symbols transport L1-pre data and L1-post data, which contain the transmission information. The data symbols carry PLPs. The P1 symbol, which is not an ordinary OFDM symbol, is used for time and frequency synchronization purpose and is inserted later. The modulation and code rate of the L1-pre data is BPSK 1/2. The L1-post data can be modulated by BPSK, quaternary phase-shift keying (QPSK), 16-QAM, or 64-QAM. The code rate is always 1/2. Each PLP has its own modulation, code rate, and interleaving depth. The modulation used by each PLP can be chosen from QPSK, 16-QAM, 64-QAM, or 256-QAM.

Fig. 3 shows the mapping of L1-pre data, L1-post data, and PLPs into a T2-frame. The L1-pre data and L1-post data are mapped to P2 symbols row-wise in a zigzag manner, while the PLPs are mapped sequentially into contiguous ranges of data symbols. Note that the L1-pre data occupies 1840 data samples in a T2-frame. The Alamouti encoding is applied to pairs of data samples in an OFDM symbol. Given an OFDM symbol $\mathbf{X} = [X_0, X_1, \ldots, X_{D-2}, X_{D-1}]^T$, unmodified OFDM symbol $\mathbf{X}_1 = [X_0, X_1, \ldots, X_{D-2}, X_{D-1}]^T$ is directed to transmitter 1 and modified OFDM symbol $\mathbf{X}_2 = [-X_1^*, X_0^*, \ldots, -X_{D-1}^*, X_{D-2}^*]^T$ are conveyed to transmitter 2, where X_n and D denote the n-th data sample and the number of data samples in one OFDM symbol, respectively. Then, five different types of pilots—P2, scatter, continual, edge, and frame closing pilots—are inserted at regular intervals between data samples. After a series of inverse fast Fourier transform (IFFT), guard interval insertion, and P1 symbol insertion, the signals are transmitted simultaneously from two distinct transmitters (see **Fig.5-(a)**).

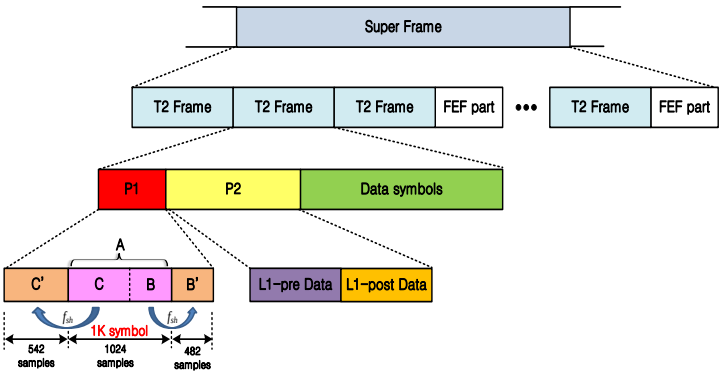

Fig. 2. Frame structure of DVB-T2 [1]

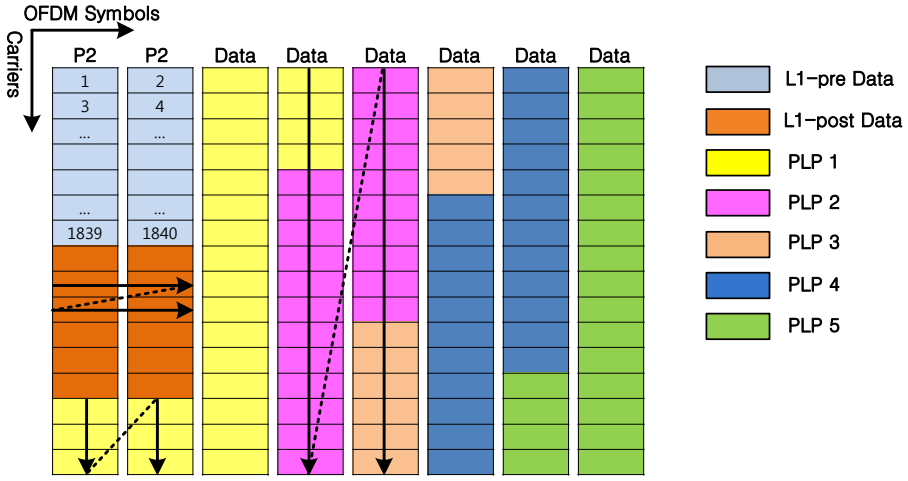

Fig. 3.. Mapping of L1-pre data, L1-post data, and PLPs [1]

2.2 Received Signal Model

A time domain OFDM symbol transmitted from each transmitter can be expressed as

$$x_n[m]=\sum_{k=0}^{N-1} X_{k,n} e^{j2\pi k\frac{m}{N}}, \quad -N_g \le m \le N-1, \tag{1}$$

where $X_{k,n}$, $k \in \{1, \ldots, N\}$, $n \in \{1, 2\}$ is a Alamouti-encoded data sample (or a pilot) at the k-th subcarrier on the n-th transmitter and N denotes the number of subcarriers in one OFDM symbol. N_g is the length of cyclic prefix (CP).

Due to the frequency mismatch between oscillators in the transmitter and the receiver and/or Doppler shift, dual CFOs are induced into the received signal. Assuming perfect timing synchronization, the received OFDM symbol can be expressed as

$$y[m]=\sum_{n=1}^{2} e^{j2\pi f_f^{(n)}\frac{m}{N}} \sum_{l=0}^{L-1} h_n[l]x_n[m-l]+n[m], \tag{2}$$

where $f_f^{(n)}$, $n \in \{1, 2\}$, is a normalized CFO (i.e., the ratio of the actual CFO to the subcarrier spacing) associated with the n-th transmitter. $h_n[l]$ denotes the channel impulse response of the l-th tap, $l \in \{0, \ldots, L\text{-}1\}$. Here we assume that CP length N_g is no less than the maximum of channel delay spread L, i.e., $L \le N_g$. We also assume that the channel is quasi-static fading channel, i.e., the channel tap do not change during one OFDM symbol, and vary independently from one OFDM symbol to another. The average total channel power is normalized such that $E\left\{\sum_{n=1}^{2}\sum_{l=0}^{L-1}|h_n(l)|^2\right\}=1$. $n[m]$ is the additive white Gaussian noise (AWGN) with a zero mean and variance of σ^2.

Let f_c represent the CFO compensation frequency. After performing the CFO compensation to the received OFDM symbol, we have

$$y[m]e^{\frac{-j2\pi f_c m}{N}} \triangleq \tilde{y}[m] = \sum_{n=1}^{2} e^{j2\pi\left(f_f^{(n)}-f_c\right)\frac{m}{N}} \sum_{l=0}^{L-1} h_n[l]x_n[m-l]+\tilde{n}[m]. \tag{3}$$

After removing the CP and performing FFT, the p-th data sample (or a pilot) can be expressed as

$$\begin{aligned} Y_p &= \frac{1}{N}\sum_{m=0}^{N-1}\tilde{y}[m]e^{\frac{-j2\pi pm}{N}} \\ &= X_{p,1}H_{p,1}\Lambda_{p,p}^{(1)} + X_{p,2}H_{p,2}\Lambda_{p,p}^{(2)} + \sum_{k=0,k\neq p}^{N-1} X_{k,1}H_{k,1}\Lambda_{k,p}^{(1)} + \sum_{k=0,k\neq p}^{N-1} X_{k,2}H_{k,2}\Lambda_{k,p}^{(2)} + N_p, \end{aligned} \tag{4}$$

where $H_{k,n}$, is channel frequency response, N_p is the FFT of the AWGN corresponding to the p-th subcarrier, and

$$\begin{aligned} \Lambda_{k,p}^{(n)} &= \frac{1}{N}\sum_{m=0}^{N-1} e^{j2\pi\left(k+(f_f^{(n)}-f_c)-p\right)\frac{m}{N}} \\ &= e^{j\pi\left(k+(f_f^{(n)}-f_c)-p\right)\frac{N-1}{N}} \frac{\sin\left(\pi(k+(f_f^{(n)}-f_c)-p)\right)}{N\sin\left(\pi(k+(f_f^{(n)}-f_c)-p)/N\right)}. \end{aligned} \tag{5}$$

On the right-hand side of (4), the first two terms contain the desired data and the remaining terms are ICI and noise. Thus, in the case of dual CFOs, there always exists ICI, no matter how the CFO compensation is performed.

2.3 Optimal Dual CFOs Compensation

In [17], the optimal compensation frequency has been mathematically derived that minimizes the power of ICI. This frequency corresponds approximately to the point that internally divides the line segment connecting $f_f^{(1)}$ and $f_f^{(2)}$ in the ratio of $s_{H,2}^2 : s_{H,1}^2$, where $s_{H,n}^2, n$ Ĭ {1, 2}, is the variance of $H_{k,n}$ for all k. This can be written as

$$f_c \simeq \frac{\sigma_{H,1}^2 f_f^{(1)} + \sigma_{H,2}^2 f_f^{(2)}}{\sigma_{H,1}^2 + \sigma_{H,2}^2}, \tag{6}$$

It can be seen from (6) that the dual CFOs, $f_f^{(1)}$ and $f_f^{(2)}$, are required to estimate the optimal compensation frequency. However, it is practically impossible for DVB-T2 system to estimate the dual CFOs when the two P1 symbols are received concurrently. A scheme is also proposed in [17] that achieves the optimal compensation frequency without requiring dual CFOs estimates. The scheme iteratively adjusts the initial compensation frequency to the optimal compensation frequency based on the measurement of the ICI-plus-noise power. Here the initial compensation frequency is obtained by correlating the sum of two concurrently received P1 symbols and by taking the argument of the correlator output' peak as described in

[2]. We employ this scheme in this paper to compensate dual CFOs (see **Fig. 5-(b)**).

3. Iterative Data Detection with Dual Phase Errors Compensation

3.1 Effect of Dual CFOs on Desired Data

After performing the CFO compensation, pilots are removed from the received T2-frame. Let Δ denote a set of data-bearing subcarriers in one OFDM symbol. Let $\{(X_{p,1}, X_{q,1}), (X_{p,2}, X_{q,2})\}$, $\{p, q\} \in \Delta$ be an Alamouti coding block, i.e., $X_{p,2} = -X^*_{q,1}$ and $X_{q,2} = X^*_{p,1}$. Then, a pair of received data samples, Y_p and Y_q, can be expressed as

$$Y_p = X_{p,1}H_{p,1}\Lambda^{(1)}_{p,p} - X^*_{q,1}H_{p,2}\Lambda^{(2)}_{p,p} + \sum_{k=0,k\neq p}^{N-1} X_{k,1}H_{k,1}\Lambda^{(1)}_{k,p} + \sum_{k=0,k\neq p}^{N-1} X_{k,2}H_{k,2}\Lambda^{(2)}_{k,p} + N_p, \quad (7)$$

$$Y_q = X_{q,1}H_{q,1}\Lambda^{(1)}_{q,q} + X^*_{p,1}H_{q,2}\Lambda^{(2)}_{q,q} + \sum_{k=0,k\neq q}^{N-1} X_{k,1}H_{k,1}\Lambda^{(1)}_{k,q} + \sum_{k=0,k\neq q}^{N-1} X_{k,2}H_{k,2}\Lambda^{(2)}_{k,q} + N_q. \quad (8)$$

The first terms on the right-hand side of (7) and (8) contain the desired data, $X_{p,1}H_{p,1}$ and $X_{q,1}H_{q,1}$, which are sent from transmitter 1. From these terms, we see that the magnitude of the desired data is attenuated by

$$\left|\Lambda^{(1)}_{p,p}\right| = \left|\Lambda^{(1)}_{q,q}\right| = \frac{\sin\left(\pi(f_f^{(1)} - f_c)\right)}{N\sin\left(\pi(f_f^{(1)} - f_c)/N\right)} \triangleq \left|\Lambda^{(1)}_0\right|, \quad (9)$$

and the phase of both terms is shifted by

$$\angle\Lambda^{(1)}_{p,p} = \angle\Lambda^{(1)}_{q,q} = \pi(f_f^{(1)} - f_c)(1-1/N) \triangleq \angle\Lambda^{(1)}_0. \quad (10)$$

Similarly, the second terms on the right-hand side of (7) and (8) contain the desired data, $X^*_{q,1}H_{p,2}$ and $X^*_{p,1}H_{q,2}$, which are sent from transmitter 2. Magnitude attenuation and phase shift for the desired data are given respectively as

$$\left|\Lambda^{(2)}_{p,p}\right| = \left|\Lambda^{(2)}_{q,q}\right| = \frac{\sin\left(\pi(f_f^{(2)} - f_c)\right)}{N\sin\left(\pi(f_f^{(2)} - f_c)/N\right)} \triangleq \left|\Lambda^{(2)}_0\right|, \quad (11)$$

$$\angle\Lambda^{(2)}_{p,p} = \angle\Lambda^{(2)}_{q,q} = \pi(f_f^{(2)} - f_c)(1-1/N) \triangleq \angle\Lambda^{(2)}_0. \quad (12)$$

In our work, we assume that both transmitter-receiver paths have the same attenuation, i.e., $s^2_{H,1} = s^2_{H,2}$. Then, according to (6) in the previous section, the optimal compensation frequency that minimizes the intensity of the ICI is given by

$$f_c \simeq \frac{f_f^{(1)} + f_f^{(2)}}{2}, \tag{13}$$

and the scheme proposed in [17] iteratively adjusts the compensation frequency to (13) based on the measurement of the ICI-plus-noise power. After the compensation frequency is optimized to (13), the magnitude attenuation and phase shift of the desired data from each transmitter have the following relationships:

$$\left|\Lambda_0^{(1)}\right| = \left|\Lambda_0^{(2)}\right| \simeq \frac{\sin\left(\pi(f_f^{(1)} - f_f^{(2)})\right)}{N\sin\left(\pi(f_f^{(1)} - f_f^{(2)})/N\right)}, \tag{14}$$

$$\angle\Lambda_0^{(1)} = -\angle\Lambda_0^{(2)} \simeq \pi/2(f_f^{(1)} - f_f^{(2)})(1-1/N), \tag{15}$$

that is,

$$\Lambda_0^{(1)} \simeq \left(\Lambda_0^{(2)}\right)^*. \tag{16}$$

This result allows us to estimate the magnitude attenuation and phase shift in the desired data. Such variations in the desired data, denoted by $\Lambda_0^{(n)}$, $n \in \{1, 2\}$, are referred to as *dual phase errors*[1].

3.2 Estimation of Dual Phase Errors

Let us define $\mathbf{Y}_{[p,q]} \triangleq [Y_p,\ Y_q^*]^T$. Then, from (16), we can represent (7) and (8) by a vector as

$$\mathbf{Y}_{[p,q]} = \tilde{\mathbf{H}}_{[p,q]}\mathbf{X}_{[p,q]} + \mathbf{W}_{[p,q]} + \mathbf{N}_{[p,q]}, \tag{17}$$

where $\mathbf{X}_{[p,q]}=[X_{p,1},\ X_{q,1}^*]^T$, $\mathbf{N}_{[p,q]}=[N_p,\ N_q^*]^T$, and

$$\tilde{\mathbf{H}}_{[p,q]} \simeq \mathbf{H}_{[p,q]}\mathbf{\Lambda}, \tag{18}$$

$$\mathbf{W}_{[p,q]} = \begin{bmatrix} \sum_{k=0,k\neq p}^{N-1} X_{k,1}H_{k,1}\Lambda_{k,p}^{(1)} + \sum_{k=0,k\neq p}^{N-1} X_{k,2}H_{k,2}\Lambda_{k,p}^{(2)} \\ \sum_{k=0,k\neq q}^{N-1} X_{k,1}^*H_{k,1}^*\Lambda_{k,q}^{(1)*} + \sum_{k=0,k\neq q}^{N-1} X_{k,2}^*H_{k,2}^*\Lambda_{k,q}^{(2)*} \end{bmatrix}. \tag{19}$$

Here, $\mathbf{H}_{[p,q]} = \begin{bmatrix} H_{p,1} & -H_{p,2} \\ H_{q,2}^* & H_{q,1}^* \end{bmatrix}$ and $\mathbf{\Lambda} = \begin{bmatrix} \Lambda_0^{(1)} & 0 \\ 0 & \Lambda_0^{(1)*} \end{bmatrix}$. From (18), we see that the matrix of dual phase errors, $\mathbf{\Lambda}$, is separated from $\tilde{\mathbf{H}}_{[p,q]}$ owing to the result of (16). Because the OFDM channel estimator has been considered in many papers, e.g., [18]][19][20], the channel

[1] The term 'phase error' is commonly referred to as '*common* phase error' because it causes equal phase shifts in all subcarriers, being independent of a particular subcarrier [14], [16].

frequency response, $\mathbf{H}_{[p,q]}$, $\{p, q\} \in \Delta$, is assumed to be known in this paper. However, the dual phase errors have to be estimated. The dual phase errors can be estimated as follows. By applying the inverse of matrix $\mathbf{H}_{[p,q]}$ to (17), we have

$$\mathbf{Z}_{[p,q]} \triangleq \mathbf{H}_{[p,q]}^{-1}\mathbf{Y}_{[p,q]} = \mathbf{\Lambda}\mathbf{X}_{[p,q]} + \underbrace{\mathbf{H}_{[p,q]}^{-1}\mathbf{W}_{[p,q]} + \mathbf{H}_{[p,q]}^{-1}\mathbf{N}_{[p,q]}}_{\triangleq \tilde{\mathbf{N}}_{[p,q]}}. \tag{20}$$

From the central limit theorem, the element in the noise signal vector, $\tilde{\mathbf{N}}_{[p,q]}$, can be a zero-mean Gaussian random variable [21]. Thus, the average of a sufficiently large number of these elements approaches zero. In addition, $\mathbf{X}_{[p,q]}$ is the vector of *unknown* data samples. By expanding (20), we have

$$\begin{cases} Z_p = \Lambda_0^{(1)} X_{p,1} + \tilde{N}_p \\ Z_q = \Lambda_0^{(1)*} X_{q,1}^* + \tilde{N}_q \end{cases}. \tag{21}$$

Note that in a T2-frame, $D_{\text{L1-pre}}$ (=1840) BPSK-modulated data samples are present, which carry the L1-pre data. Because the BPSK signal is highly robust against false detection, it can act like the pilot signal. For the L1-pre data, (21) is reduced to

$$\begin{cases} Z_p = \pm\Lambda_0^{(1)} + \tilde{N}_p \\ Z_q = \pm\Lambda_0^{(1)*} + \tilde{N}_q \end{cases}. \tag{22}$$

Let $D_{p,\text{L1-pre}}$ and $D_{q,\text{L1-pre}}$ denote the number of BPSK-modulated data samples corresponding to $X_{p,1}$ and $X_{q,1}^*$, respectively, i.e., $D_{p,\text{L1-pre}} + D_{q,\text{L1-pre}} = D_{\text{L1-pre}}$. Then, the estimates of $\Lambda_0^{(1)}$ and $\Lambda_0^{(1)*}$ can be obtained respectively as

$$\hat{\Lambda}_0^{(1)} = \frac{\sum_p Z_p^+ - Z_p^-}{D_{p,\text{L1-pre}}}, \tag{23}$$

$$\hat{\Lambda}_0^{(1)*} = \hat{\Lambda}_0^{(2)} = \frac{\sum_q Z_q^+ - Z_q^-}{D_{q,\text{L1-pre}}}, \tag{24}$$

where Z_k^+ (or Z_k^-) for $k \in \{p, q\}$ is equal to Z_k, for which the real part of Z_k has a positive (or a negative) value. The block diagram of the dual phase errors estimator is shown in **Fig. 4**.

3.3 MAP Detection with Dual Phase Errors Compensation

Recall that the T2-frame consists of data samples of PLPs and every PLP has its own

modulation. Let M_p and M_q represent the modulation order (i.e., the number of bits per constellation) for $X_{p,1}$ and $X^*_{q,1}$ respectively. Let $\mathbf{x} = [x_1, x_2, \ldots, x_{2^{Mp+Mq}}]^T$ also denote the bit sequence mapped to $\mathbf{X}_{[p,q]}$. Given $\mathbf{H}_{[p,q]}$, $\hat{\mathbf{\Lambda}}$, and s^2, the log-likelihood ratio (LLR) of x_i, iÏ {0,…, 2^{Mp+Mq}-1} estimated using a mutiple-input mutiple-output (MIMO) *maximum a posteriori* (MAP) detector is written as [22], [23]

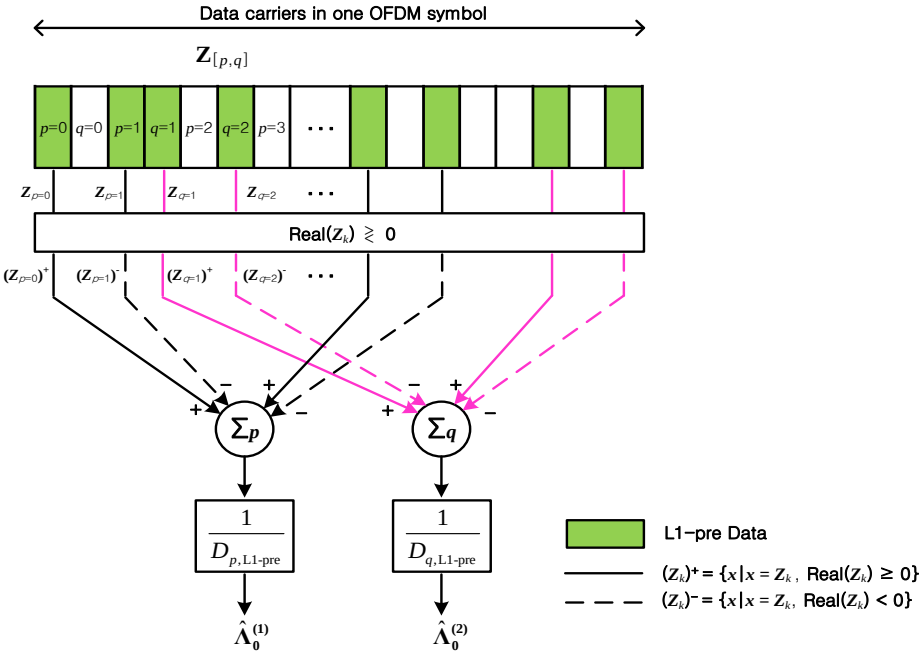

Fig. 4. Block diagram of proposed dual phase errors estimator

$$LLR(x_i \mid \mathbf{Y}_{[p,q]}) = \log \frac{\Pr\left(x_i = 0 \mid \mathbf{Y}_{[p,q]}, \mathbf{H}_{[p,q]}, \hat{\mathbf{\Lambda}}, s^2\right)}{\Pr\left(x_i = 1 \mid \mathbf{Y}_{[p,q]}, \mathbf{H}_{[p,q]}, \hat{\mathbf{\Lambda}}, s^2\right)}. \tag{25}$$

By applying the max-log approximation to (25), we can calculate the *extrinsic* LLR value as

$$\begin{aligned} L_E(x_i \mid \mathbf{Y}_{[p,q]}) \simeq & \frac{1}{2} \max_{\mathbf{b} \in \mathcal{B}_{i=1}} \left\{ \frac{1}{\sigma^2} \left\| \mathbf{Y}_{[p,q]} - \mathbf{H}_{[p,q]} \hat{\mathbf{\Lambda}} \mathbf{s} \right\|^2 - \left(2\mathbf{b}_{[i]} - 1\right)^T \cdot L_{A,[i]}(\mathbf{b}) \right\} \\ & - \frac{1}{2} \max_{\mathbf{b} \in \mathcal{B}_{i=0}} \left\{ \frac{1}{\sigma^2} \left\| \mathbf{Y}_{[p,q]} - \mathbf{H}_{[p,q]} \hat{\mathbf{\Lambda}} \mathbf{s} \right\|^2 - \left(2\mathbf{b}_{[i]} - 1\right)^T \cdot L_{A,[i]}(\mathbf{b}) \right\}, \end{aligned} \tag{26}$$

where $\hat{\mathbf{\Lambda}} = \begin{bmatrix} \hat{\Lambda}_0^{(1)} & 0 \\ 0 & \hat{\Lambda}_0^{(1)*} \end{bmatrix}$. Here, $\mathcal{B}_{i=0}$ and $\mathcal{B}_{i=1}$ are the set of all possible bit sequences **b**, for which the *i*-th bit is 0 and 1, respectively. In addition, **s** is the constellation vector obtained by mapping **b**, and $\mathbf{b}_{[i]}$ denotes a subvector of **b** from which the *i*-th element is omitted. $L_{A,[i]}(\mathbf{b})$ is the vector of the *a priori* LLR value corresponding to $\mathbf{b}_{[i]}$. Here, the *a priori* LLR value of each bit is defined as

$$L_A(b_i) \triangleq \log \frac{\Pr(b_i = 0)}{\Pr(b_i = 1)}, \tag{27}$$

which is equal to the *extrinsic* LLR value fed back from the LDPC decoder.

4. Iterative Data Detection and ICI Cancellation

In this section, we consider a DVB-T2 iterative receiver employing the successive-iterative ICI cancellation technique. The proposed technique consists of max-log MAP detection with the dual phase errors compensation technique, successive ICI cancellation for the first iteration, and iterative ICI cancellation for subsequent iterations.

4.1 Successive ICI Cancellation

The concept behind the successive cancellation (SC) method is similar to the well-known vertical Bell Laboratories layered space-time (V-BLAST) scheme for MIMO detection [24], [25]. The SC method eliminates ICI caused by pre-detected data samples before the detection of the next unresolved data. After reconstructing the ICI caused by the pre-detected data samples, the corresponding interference is cancelled out. Then, the next detection is performed, and so on. The procedure continues *successively* until all the data samples in an OFDM symbol are detected.

In Section 3.2, (19) represents the vector of ICI. Here, note that the coefficients $\mathrm{L}_{k,p}^{(n)}$, $k \in \{0,1,\ldots,N\text{-}1\}\backslash\{p\}$, and $\mathrm{L}_{k,q}^{(n)}$, $k \in \{0,1,\ldots, N\text{-}1\}\backslash\{q\}$, for $n \in \{1, 2\}$ are unknown since the estimates of dual CFOs are not given to the receiver. In order to reconstruct the ICI, these coefficients need to be estimated. Fortunately, these coefficients can be approximated as a function of dual phase errors. For DVB-T2, the FFT-size, N, can be 1K, 2K, 4K, 8K, 16K, or 32K, where K = 1024. For these FFT-size values, (15) in Section 3.1 can be well approximated as

$$\angle\Lambda_0^{(1)} \simeq \pi/2\,(f_f^{(1)} - f_f^{(2)}). \tag{28}$$

Then, denoting $\lambda \triangleq \angle\Lambda_0^{(1)}/\pi$, the approximation of $\mathrm{L}_{k,a}^{(1)}$ for $a \in \{p, q\}$, $k \in \{0,1,\ldots,N\text{-}1\}\backslash\{a\}$, can be derived as a function of λ as

$$\begin{aligned}
\Lambda_{k,a}^{(1)} &= e^{j\pi\left(k+(f_f^{(1)}-f_c)-a\right)\frac{N-1}{N}} \left.\frac{\sin\left(\pi(k+(f_f^{(1)}-f_c)-a)\right)}{N\sin\left(\pi(k+(f_f^{(1)}-f_c)-a)/N\right)}\right|_{f_c=\left(f_f^{(1)}+f_f^{(2)}\right)/2} \\
&\simeq e^{j\pi\left(k+(f_f^{(1)}-f_f^{(2)})/2-a\right)} \frac{\sin\left(\pi(k+(f_f^{(1)}-f_f^{(2)})/2-a)\right)}{N\sin\left(\pi(k+(f_f^{(1)}-f_f^{(2)})/2-a)/N\right)} \\
&= e^{j\pi(k+\lambda-a)} \frac{\sin\left(\pi(k+\lambda-a)\right)}{N\sin\left(\pi(k+\lambda-a)/N\right)},
\end{aligned} \tag{29}$$

and similarly, the approximation of $\mathrm{L}_{k,a}^{(2)}$ for $a \in \{p, q\}$, $k \in \{0,1,\ldots,N\text{-}1\}\backslash\{a\}$, can also be derived as a function of λ as

$$\Lambda_{k,a}^{(2)} \simeq e^{j\pi(k-\lambda-a)} \frac{\sin\left(\pi(k-\lambda-a)\right)}{N\sin\left(\pi(k-\lambda-a)/N\right)}. \tag{30}$$

Therefore, by using the estimated dual phase errors $\hat{\mathrm{L}}_0^{(1)}$ from (23), we can obtain estimates of (29) and (30), which are denoted as $\hat{\mathrm{L}}_{k,a}^{(n)}$ for a Ï {p, q}, kÏ {0,1,…, N-1}\{a}, nÏ {1, 2}, by substituting $\hat{\lambda} = \angle\hat{\Lambda}_0^{(1)}/\pi$ into (29) and (30).

Now, we are ready to reconstruct the ICI caused by pre-detected data samples. From (26) in Section 3.3, the *extrinsic* LLR values of $\mathbf{X}_{[p,q]}$, calculated by max-log MAP detection can be represented as

$$\mathbf{L}_E^{[p,q]} \triangleq \left[L_E(x_0 \mid \mathbf{Y}_{[p,q]}),\ L_E(x_1 \mid \mathbf{Y}_{[p,q]}),\ \ldots,\ L_E(x_{2^{Mp+Mq}-1} \mid \mathbf{Y}_{[p,q]})\right]^T. \tag{31}$$

Then, we can estimate x_i for iÏ {0,…, 2^{Mp+Mq}-1} by hard-deciding (31) as

$$\hat{x}_i = \begin{cases} 0 & \text{if } L_E(x_i \mid \mathbf{Y}_{[p,q]}) > 0 \\ 1 & \text{else} \end{cases}. \tag{32}$$

After re-modulating $\hat{x}_i$, we can obtain the estimate for $\hat{\mathbf{X}}_{[p,q]} = [\hat{X}_{p,1}, \hat{X}_{q,1}^*]^T$ corresponding to (31). Let $\{p^+, q^+\}$Ï Δ denote a pair of data indexes for the next detection. Let D_a also denote the set of pre-detected data indexes until the a-th data pair, defined by $D_a = \{i \mid i$ 誇D, i $a\}$. Before the detection of next data pair $\mathbf{Y}_{[p^+,q^+]}$, the interference caused by $\hat{\mathbf{X}}_{[p,q]}$ is eliminated as

$$\tilde{\mathbf{Y}}_{[p^+,q^+]} \triangleq \mathbf{Y}_{[p^+,q^+]} - \tilde{\mathbf{W}}_{[p,q]} = \begin{bmatrix} Y_{p^+} \\ Y_{q^+}^* \end{bmatrix} - \begin{bmatrix} \sum_{k\in\mathcal{D}_p} \hat{X}_{k,1} H_{k,1} \hat{\Lambda}_{k,p}^{(1)} + \sum_{k\in\mathcal{D}_p} \hat{X}_{k,2} H_{k,2} \hat{\Lambda}_{k,p}^{(2)} \\ \sum_{k\in\mathcal{D}_q} \hat{X}_{k,1}^* H_{k,1}^* \hat{\Lambda}_{k,q}^{(1)*} + \sum_{k\in\mathcal{D}_q} \hat{X}_{k,2}^* H_{k,2}^* \hat{\Lambda}_{k,q}^{(2)*} \end{bmatrix}, \tag{33}$$

and the next detection is carried out from the refined data pair $\tilde{\mathbf{Y}}_{[p^+,q^+]}$. The procedure of max-log MAP detection combined with the dual phase errors compensation given in (26) and ICI cancellation given in (31), (32), and (33) is repeated until all the data samples in an OFDM symbol are detected. This enables the following LDPC decoder to produce reliable *a priori* information in the first iteration.

4.2 Iterative ICI Cancellation

It is well known that significant coding gain is obtained by applying LDPC decoding. The *a priori* LLR value, defined by (27) in Section 3.3, is fed from the LDPC decoder, and it can be used to accurately cancel out ICI. However, in the first iteration, the *a priori* LLR values are initialized to zero; thus the ICI cannot be eliminated. This makes the following max-log MAP detection unreliable. The erroneous detection of a data pair leads to error propagation in the SC method. To solve this problem, we use pilots for the initial cancelling of the ICI. Let Π denote a set of pilot subcarriers in one OFDM symbol. Then, for the received data pairs $\mathbf{Y}_{[p,q]}$ defined by (17) in Section 3.2, the ICI caused by the pilots is first eliminated as

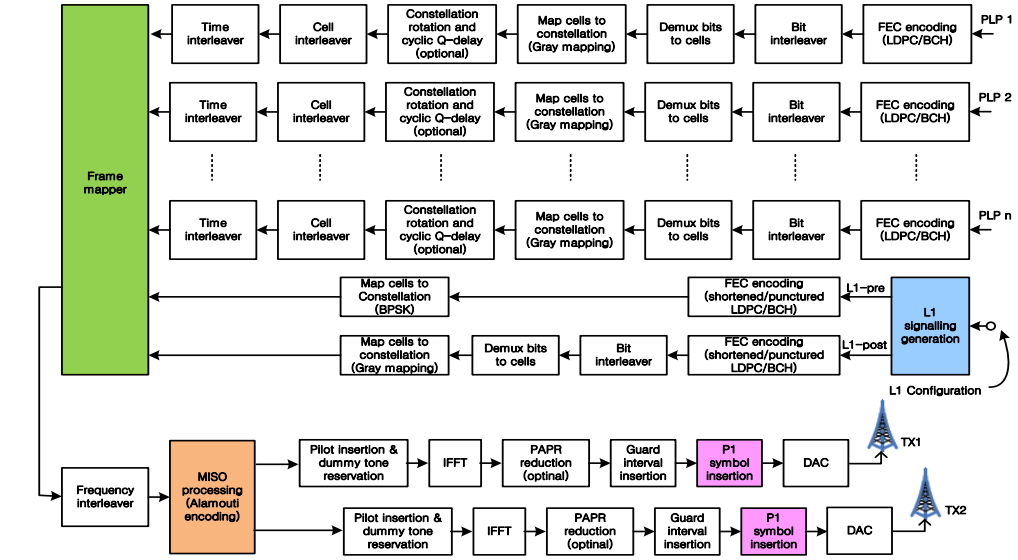

(a)

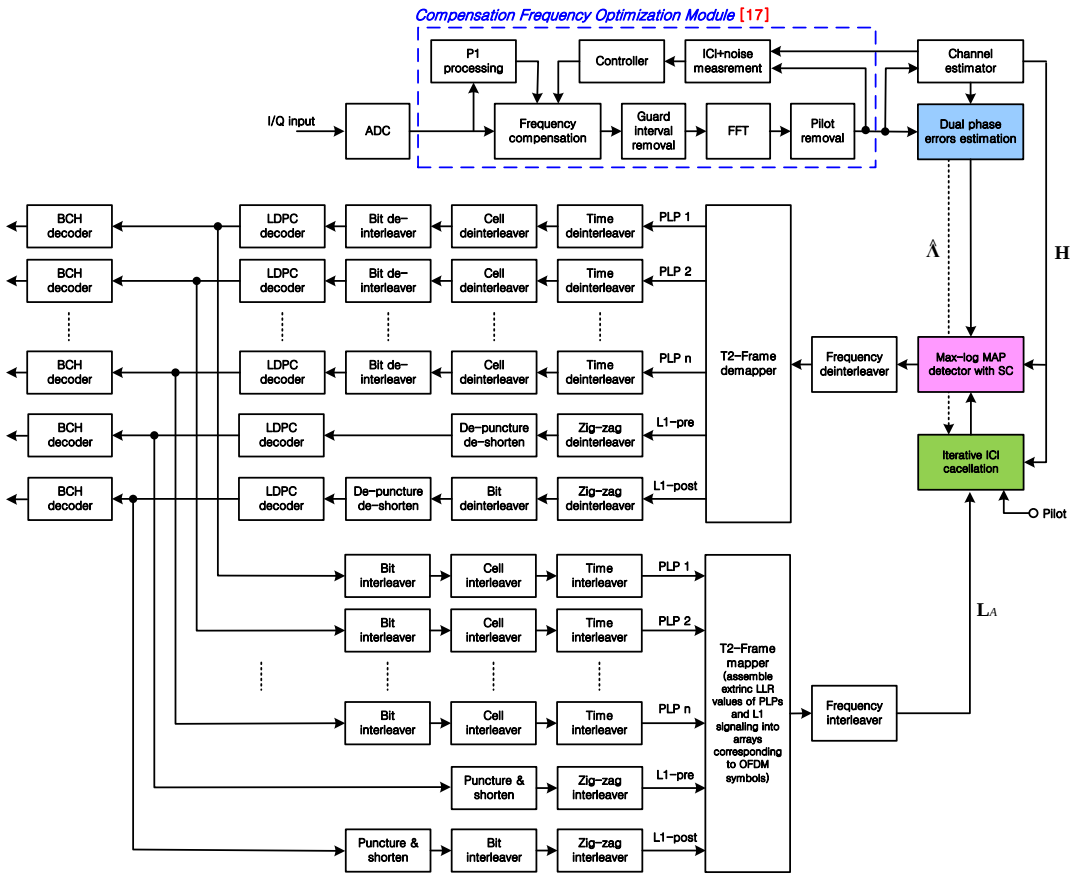

(b)

Fig. 5. Block diagram of MISO-mode DVB-T2 system: (a) MISO-mode transmitter, (b) iterative receiver with proposed scheme

$$\tilde{\mathbf{Y}}^{(0)}_{[p,q]} \triangleq \mathbf{Y}_{[p,q]} - \mathbf{P}_{[p,q]} = \begin{bmatrix} Y_p \\ Y^*_q \end{bmatrix} - \begin{bmatrix} \sum_{k\in\mathcal{P}} P_{k,1} H_{k,1} \hat{\Lambda}^{(1)}_{k,p} + \sum_{k\in\mathcal{P}} P_{k,2} H_{k,2} \hat{\Lambda}^{(2)}_{k,p} \\ \sum_{k\in\mathcal{P}} P_{k,1} H^*_{k,1} \hat{\Lambda}^{(1)*}_{k,q} + \sum_{k\in\mathcal{P}} P_{k,2} H^*_{k,2} \hat{\Lambda}^{(2)*}_{k,q} \end{bmatrix}, \quad (34)$$

where $P_{k,n}$ denotes the pilot for subcarrier k in the n-th transmitter. Then, max-log MAP detection combined with the dual phase errors compensation is applied to $\tilde{\mathbf{Y}}^{(0)}_{[p,q]}$ in conjunction with the SC method, as described in the previous section. After LDPC decoding, the *a priori* LLR values of each bit are available as

$$\mathbf{L}_A \triangleq \left[L_A(b_0), L_A(b_1), \ldots, L_A(b_{N_{ldpc}-1}) \right]^T, \quad (35)$$

where N_{ldpc} is the number of bits in an LDPC decoding block. After a series of hard decisions for (35), re-modulation, and Alamouti encoding, we can re-generate Alamouti coding pair $\hat{\mathbf{X}}_{[p,q]} = [\hat{X}_{p,1}, \hat{X}^*_{q,1}]^T$ corresponding to (35). Thus, from the second iteration onward, the ICI caused by both the pilots and other data samples can be subtracted from $\mathbf{Y}_{[p,q]}$ as

$$\begin{aligned} \tilde{\mathbf{Y}}^{(l)}_{[p,q]} &= \mathbf{Y}_{[p,q]} - \mathbf{P}_{[p,q]} - \tilde{\tilde{\mathbf{W}}}_{[p,q]} \\ &= \begin{bmatrix} Y_p \\ Y^*_q \end{bmatrix} - \begin{bmatrix} \sum_{k\in\mathcal{P}} P_{k,1} H_{k,1} \hat{\Lambda}^{(1)}_{k,p} + \sum_{k\in\mathcal{P}} P_{k,2} H_{k,2} \hat{\Lambda}^{(2)}_{k,p} \\ \sum_{k\in\mathcal{P}} P_{k,1} H^*_{k,1} \hat{\Lambda}^{(1)*}_{k,q} + \sum_{k\in\mathcal{P}} P_{k,2} H^*_{k,2} \hat{\Lambda}^{(2)*}_{k,q} \end{bmatrix} - \begin{bmatrix} \sum_{k\in\mathcal{D}\setminus\{p\}} \hat{X}_{k,1} H_{k,1} \hat{\Lambda}^{(1)}_{k,p} + \sum_{k\in\mathcal{D}\setminus\{p\}} \hat{X}_{k,2} H_{k,2} \hat{\Lambda}^{(2)}_{k,p} \\ \sum_{k\in\mathcal{D}\setminus\{q\}} \hat{X}^*_{k,1} H^*_{k,1} \hat{\Lambda}^{(1)*}_{k,q} + \sum_{k\in\mathcal{D}\setminus\{q\}} \hat{X}^*_{k,2} H^*_{k,2} \hat{\Lambda}^{(2)*}_{k,q} \end{bmatrix} \end{aligned} \quad (36)$$

and the max-log MAP detection combined with the dual phase errors compensation is performed to the refined data $\tilde{\mathbf{Y}}^{(l)}_{[p,q]}$ of (36) for l=1,2,….

5. Performance Evaluation

In this section, we evaluate the performance of the proposed schemes in terms of the bit error rate (BER). We carried out Monte Carlo simulations using a full DVB-T2 simulator shown in **Fig. 5**. The basic simulation parameters are listed in **Table 1**. Parameters basically follow the DVB-T2 standard, and the modulation of QPSK and 16-QAM were adopted to evaluate the trends of BER performance according to the various dual CFOs. For channel model, the MISO channel described in implementation guideline [2] is adopted, which is generally used to describe the portable indoor or outdoor reception conditions. The channel did not include any Doppler and should therefore be considered as a snapshot of the real time-variant channel. The channel frequency responses $H_{k,n}$ were assumed to be perfectly known at the receiver. Both transmitted signals were assumed to have nearly same strength at the reception site, arriving at the same time with different CFOs. Each CFO was assumed to be fixed in the range of half the carrier spacing, i.e., $-0.5 \leq f_f^{(n)} \leq 0.5$ for $n \in \{1, 2\}$. In all simulations, the BER of a data signal in a single PLP was measured after LDPC decoding. To ensure reliable results, the

Table 1. DVB-T2 simulation parameters

Class	Parameters	Options
OFDM	FFT size	2K
	Pilot pattern	PP3
	Guard interval	1/16
	PAPR	No
	Carrier spacing	4464Hz
PLP	Number of PLPs	1
	PLP type	Common PLP
	Modulation	QPSK, 16-QAM
	FEC rate	1/2 (short frame)
	Constellation rotation	No
	Time interleaver type	Type 1
L1 signal	Modulation (L1-pre)	BPSK
	FEC rate (L1-pre)	1/4 (short frame)
	Modulation (L1-post)	QPSK
	FEC rate (L1-post)	1/2 (short frame)
General	Bandwidth	8MHz
	Carrier frequency	730MHz
	Number of LDPC iterations	50
	Channel type	MISO channel [2]
	Number of T2-frames in a super frame	2
	Number of FEC blocks in a T2-frame	10
	Number of data OFDM symbols in a T2-frame	22 (for QPSK), 12 (for 16-QAM)
	Number of P2 OFDM symbols in a T2-frame	8
	Number of AUX streams	1
	Bandwidth extension-mode	No
	Number of subslices in a T2-frame	1

For a more detailed explanation on the parameters, please refer to [1].

simulations were run until minimum of 100 erroneous forward error correction (FEC) blocks were collected. The performance of the DVB-T2 non-iterative receiver employing the proposed dual phase errors estimator was firstly investigated in **Fig. 6**. and **Fig. 7**. Then, the performance of the DVB-T2 iterative receiver with the proposed dual phase errors estimator and the successive-iterative ICI cancellation technique was evaluated in **Fig. 8**. To benchmark the performance with the proposed techniques, we considered the performance for perfectly known dual CFOs and for dual CFOs-free cases. In case of the perfectly known dual CFOs, the compensation frequency was set to optimal value given by (6) in Section 2.3 and dual phase errors were assumed to be perfectly compensated.

Fig. 6 shows the BER performance of the evaluated DVB-T2 receivers with QPSK modulation in the case of dual CFOs $f_f^{(1)} = 0.1$ and $f_f^{(2)} = 0.3$. The "Original T2" refers to the performance of the conventional DVB-T2 receiver, and "T2 with Optimized Compensation Frequency" represents the performance of the DVB-T2 receiver employing the compensation frequency optimization scheme proposed in [17]. The performance of proposed DVB-T2 receiver was obtained by jointly using the compensation frequency optimization scheme and the dual phase errors estimation. In this simulation, we did not consider the ICI cancellation technique so that we could see only the effect of the dual phase errors estimation on the performance. First, it can be seen that the conventional DVB-T2 receiver suffered large degradation in the presence of dual CFOs. The DVB-T2 receiver employing the compensation frequency optimization scheme performed better than the conventional DVB-T2 receiver, but

it is still lower than the benchmark performance. This is due to the dual phase errors in the desired data, which is proportional to the difference between the dual CFOs, i.e.,

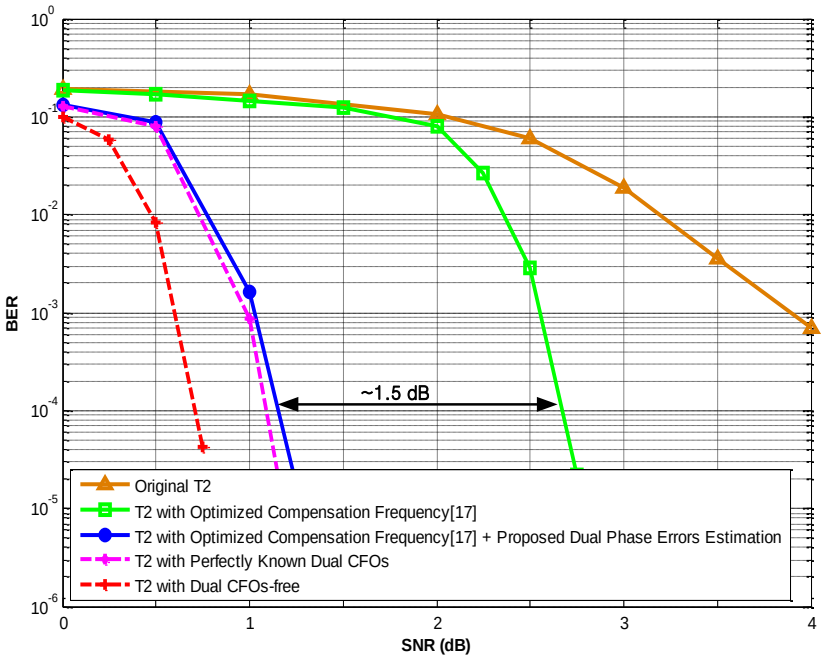

Fig. 6. BER comparison for QPSK MISO-mode DVB-T2 system with non-iterative detection in presence of dual CFOs $f_f^{(1)} = 0.1$ and $f_f^{(2)} = 0.3$.

$f_f^{(1)}$ - $f_f^{(2)}$ (refer to (14) and (15) in Section 3.1). The receiver jointly employing the compensation frequency optimization scheme and the proposed dual phase errors estimation provided almost the same performance as that of perfectly known dual CFOs.

Fig. 7 shows the BER performance of the evaluated DVB-T2 receivers with 16-QAM modulation in the case of dual CFOs $f_f^{(1)} = 0.05$ and $f_f^{(2)} = 0.35$, which have a relatively larger difference between dual CFOs than do the previous cases. In this case, both the conventional DVB-T2 receiver and the DVB-T2 receiver with the compensation frequency optimization scheme suffered from a severe error floor. This can be ascribed to the fact that the large dual phase errors in the desired data caused irrecoverable loss during the detection. The proposed DVB-T2 receiver provided no error floor and still achieved the performance with perfectly known dual CFOs. However, the performance gap between this case and the dual CFOs-free case increased to around 3dB. This can be ascribed to the fact that the ICI increased considerably owing to the increased difference in dual CFOs. However, for large dual CFOs, the proposed iterative detection and ICI cancellation technique improved the performance significantly, as shown next.

Fig. 8 shows the BER peformance of the DVB-T2 receiver with the proposed iterative detection and ICI cancellation. It is found that the proposed DVB-T2 receiver outperformed the case of perfectly known dual CFOs. Moreover, the performance loss compared with the ideal dual CFOs-free case is less than 1dB. This suggests that the proposed iterative detection and ICI cancellation is effective in supressing the ICI caused by large dual CFOs, even though the estimates of dual CFOs are not given to the receiver.

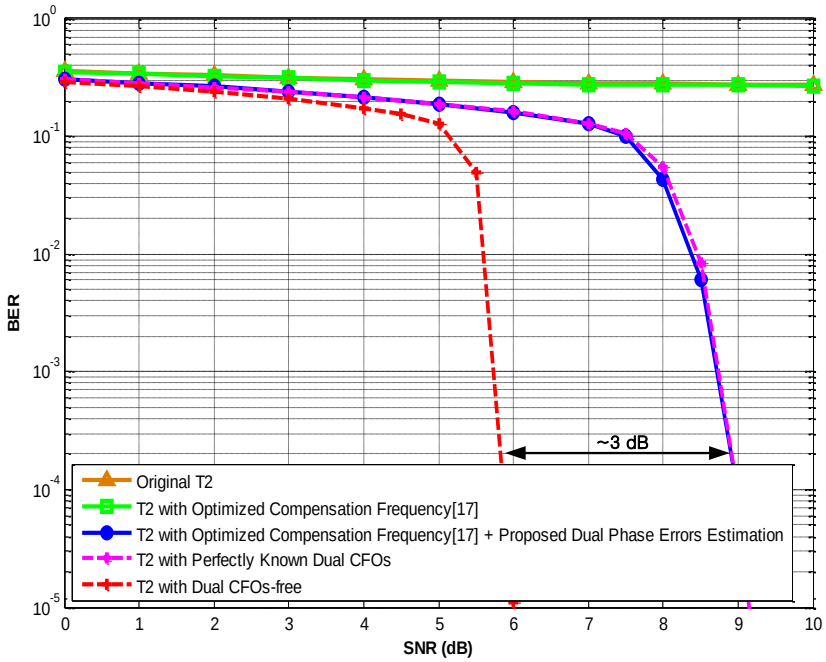

Fig. 7. BER comparison for 16-QAM MISO-mode DVB-T2 system with non-iterative detection in presence of dual CFOs $f_f^{(1)} = 0.05$ and $f_f^{(2)} = 0.35$.

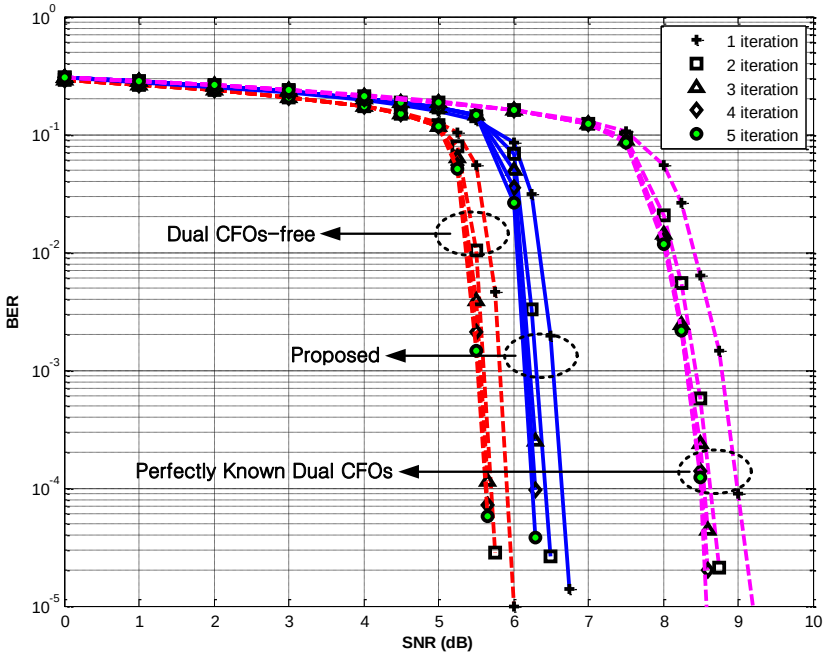

Fig. 8. BER comparison for 16-QAM MISO-mode DVB-T2 system with iterative detection and ICI cancellation in presence of dual CFOs $f_f^{(1)} = 0.05$ and $f_f^{(2)} = 0.35$.

6. Conclusion

In the presence of dual CFOs, ICI always exists even after performing dual CFOs compensation. Moreover, the phase of the desired data shifts with attenuated magnitude because of the dual phase errors. In this paper, we first proposed a technique for estimating such dual phase errors in the desired data. We used the fact that when the compensation frequency is optimized, the terms related to the dual phase errors are separated from the channel matrix. These terms were estimated using the BPSK-modulated L1-pre data. Because the ICI degrades the performance for large dual CFOs, we also proposed iterative detection and ICI cancellation technique in which the ICI is eliminated in a successive and iterative manner using the previously detected data samples and *a priori* LLR values fed from the LDPC decoder. We also found that ICI coefficients of other subcarriers, which should be estimated for ICI reconstruction, can be easily derived by using the estimated dual phase errors. Simulation results showed that the proposed DVB-T2 receiver outperforms the case in which dual CFOs are perfectly known and approaches the performance of the ideal dual CFOs-free case, even though the dual CFOs are unknown to the receiver. The proposed techniques can be applied to the current MISO-mode DVB-T2 receiver with two options: a regular DVB-T2 receiver in which only the dual phase errors estimator is used to compensate for dual phase errors or a more advanced receiver that uses iterative detection and ICI cancellation to suppress the ICI.

References

[1] ETSI, "Digital video broadcasting (DVB): Framing structure, channel coding and modulation for a second generation digital terrestrial television broadcasting system (DVB-T2)," *ETSI EN 302 755 V1.1.1*, 2009. Article (CrossRefLink)

[2] ETSI, "Implementation guidelines for a second generation digital terrestrial television broadcasting system (DVB-T2)," *DVB document A133*, Nov.2009. Article (CrossRefLink)

[3] S. Alamouti, "A simple transmit diversity technique for wireless communications," *IEEE Journal Selected Areas in Communications*, vol.16, no.8, pp.1451-1458, Oct.1998. Article (CrossRef Link)

[4] Z. Li, D. Qu and G. Zhu, "An equalization technique for distributed STBC-OFDM system with multiple carrier frequency offsets," *in Proc. of IEEE Wireless Commun. and Networking Conference*, vol.2, pp.839-843, Apr.2006. Article (CrossRefLink)

[5] Y. J. Kim, H. Lee, H. K. Chung and Y. S. Cho, "An iterative decoding technique for cooperative STBC-OFDM systems with multiple carrier frequency offsets," *in Proc. of IEEE International Symosium on Personal, Indoor and Mobile Radio Communication,* Sep.2007. Article (CrossRefLink)

[6] Q. Huang, M. Ghogho, D. Ma and J. Wei, "Low-complexity data-detection algorithm in cooperative SFBC-OFDM systems with multiple frequency offsets," *IEEE Transactions on Vehicle Technol.*, vol.59, no.9, pp.4614-4620, Nov.2010. Article (CrossRefLink)

[7] A. Ö. Yilmaz, "Cooperative diversity in carrier frequency offset," *IEEE Communicaion Letter*, vol.11, no.4, pp307-309, Apr.2007. Article (CrossRefLink)

[8] Y. Zhang and J. Zhang, "Multiple CFOs compensation and BER analysis for cooperative communication systems," *in Proc. of IEEE Wireless Communication and Networking Conference (WCNC)*, Apr.2009. Article (CrossRefLink)

[9] T.-T. Lu, H.-D. Lin and T.-H. Sang, "An SFBC-OFDM receiver to combat multiple carrier frequency offsets in cooperative communications," *in Proc. of IEEE International Symposium on Personal, Indoor and Mobile Radio Communication*, Sep.2010. Article (CrossRefLink)

[10] Z. Li and X.-G. Xia, "An Alamouti coded OFDM transmission for cooperative systems robust both timing errors and frequency offsets," *IEEE Transaction on Wireless Communication*, vol.7, no.5, May.2008. Article (CrossRefLink)

[11] Z. Li and X.-G. Xia, "A simple Alamouti space-time transmission scheme for asynchronous cooperative systems," *IEEE Signal Processing Letter*, vol.14, no.11, pp.804-807, Nov.2007. Article (CrossRefLink)
[12] H. Wang, X.-G. Xia and Q. Yin, "Distributed space-frequency codes for cooperative communication systems with multiple carrier frequency offsets," *IEEE Transactions on Wireless Communication*, vol.8, no.2, pp.1045-1055, Feb.2009. Article (CrossRefLink)
[13] X. Li, "Space-time coded multi-transmission among distributed transmitters without perfect synchronization," *IEEE Signal Processing Letter*, vol.11, no.12, pp.948-951, Dec.2004. Article (CrossRefLink)
[14] P. Robertson and S. Kaiser, "Analysis of the effect of phase noise in orthogonal frequency division multiplexing (OFDM) systems," *in Proc. of IEEE Int. Conference on Communication*, vol.3, pp.1652-1653, Jun.1995. Article (CrossRefLink)
[15] A. G. Armada and M. Calvo, "Phase noise and sub-carrier spacing effects on the performance of an OFDM communication system," *IEEE Communication Letter*, vol.2, no.1, pp.11-13, Jan.1998. Article (CrossRefLink)
[16] S. Wu and Y. Bar-Ness, "A phase noise suppression algorithm for OFDM based WLANs," *IEEE Commnication Letter*, vol.6, no.12, pp.535-537, Dec.2002. Article (CrossRefLink)
[17] E.-S. Jeon, J.-W. Seo, J.-H. Yang, J.-H. Paik and D.-K. Kim, "Optimal compensation of dual carrier frequency offsets for MISO-mode DVB-T2," *KSII Transactions on Internet and Information System*.
[18] Y. Li, N. Seshadri and S. Ariyavistitakul, "Channel estimation for OFDM systems with transmit diversity in mobile wireless channels," *IEEE Journal Selected Areas in Communication*, vol.16, no.3, pp.461-471, Mar.1999. Article (CrossRefLink)
[19] D. Qu, G. Zhu and Tao Jiang, "Training sequence design and parameter estimation of MIMO channels with carrier frequency offsets," *IEEE Transactions on Wireless Communication*, vol.5, no.12, Dec.2006. Article (CrossRefLink)
[20] J.-W. Seo, W.-G. Jeon, J.-H Paik, M. Jo and D.-K. Kim, "A composite LMMSE channel estimator for spectrum-efficient OFDM transmit diversity," *KSII Transactions on Internet and Information Systems*, vol.2, no.4, pp.209-221, Aug.2008. Article (CrossRefLink)
[21] A. Papoulis and S. U. Pillai, "Probability, Random Variables and Stochastic Processes," *McGraw-Hill*, 2002.
[22] B. M. Hochwald and S. ten Brink, "Achieving near-capacity on a multiple-antenna channel," *IEEE Transactions on Communication*, vol.51, no.3, pp.389-399, Mar.2003. Article (CrossRefLink)
[23] K. H. Kim, S. W. Kang, M. Mohaisen and K. H. Chang, "An algorithm for iterative detection and decoding MIMO-OFDM HARQ with antenna scheduling," *KSII Transactions on Internet and Information System*, vol.2, no.4, Aug.2008. Article (CrossRefLink)
[24] G. J. Foschini, "Layered space-time architecture for wireless communication in a flat fading environment when using multi-element antennas," *Bell Lab. Technology Journal*, vol.1, no.2, pp.41-59, 1996. Article (CrossRefLink)
[25] M. Mohaisen, H. An and K.-H. Chang, "Detection techniques for MIMO multiplexing: a comparative review," *KSII Transactions on Internet and Information System*, vol.3, no.6, Dec.2009. Article (CrossRefLink)

Eun-Sung Jeon received his B.S. (honors) and M.S. degrees in Electrical and Electronics Engineering from Yonsei University, Seoul, Korea, in 2005 and 2007 respectively. Since 2007, he has been in the Ph.D. program of Electrical and Electronic Engineering at Yonsei University. His main research interests include signal processing techniques for communication and broadcasting systems.

Jeong-Wook Seo received his B.S. and M.S. degrees in the Department of Telecommunication and Information Engineering from Korea Aerospace University, Gyeonggi, Korea, in 1999 and 2001, respectively and his Ph.D. in the Department of Electrical and Electronic Engineering from Yonsei University, Seoul, Korea in 2010. Since 2001, he has been with Advanced Mobile Technology Research Center in Korea Electronics Technology Institute (KETI), Gyeonggi, Korea. His research interests include statistical signal processing, digital communications, and OFDM-based wireless systems.

Jang-Hoon Yang received his Ph.D. in Electrical Engineering from University of Southern California, Los Angeles, USA, in 2001. He is currently an Assistant Professor at the Department of Newmedia, Korean German Institute of Technology, Seoul, Korea. From 2001 to 2006, he was with communication R&D center, Samsung Electronics. From 2006 to 2009, he was a Research Assistant Professor at the Department of Electrical and Electronic Engineering, Yonsei University. He has published numerous papers in the area of multi-antenna transmission and signal processing. His research interest includes wireless system and network, artificial intelligence, neuroscience, and brain computer interface.

Richard (Jong-Ho) Paik received the B.S., M.S., and Ph.D. degrees in the school of Electrical and Electronic Engineering from Chung-Ang University, Seoul, Korea, in 1994, 1997, and 2007, respectively. He was a Director with Advanced Mobile Research Center at Korea Electronics Technology Institute (KETI) by 2011. He is currently a assistant professor in the Multimedia department, Seoul Women's University, Seoul, since 2011. His research interests are in the areas of wireless/wired communications system design, video communications system design, and system architecture for realizing advanced digital communications system and for advanced mobile broadcasting networks as well.

Dong-Ku Kim received his B.S. degree from the Korea Aerospace University in 1983, and his M.S. and Ph.D. degrees from the University of Southern California, Los Angeles, in 1985 and 1992, respectively. He worked on CDMA systems in the cellular infrastructure group of Motorola, Fort Worth, TX, in 1992. He has been a Professor in the Department of Electrical and Electronic Engineering, Yonsei University, Seoul, Korea, since 1994, and was also a director of Radio Communication Research Center, Yonsei University. His research interests are cooperative MIMO and relays, interference management, compressive sensing for device to device communication, and UAV tracking.